Organic/Inorganic Langmuir−Blodgett Films Based on Metal Phosphonates: Preparation and Characterization of Phenoxy- and Biphenoxy-Substituted Zirconium Phosphonate Films

Melissa A. Petruska, Gail E. Fanucci, and Daniel R. Talham*

Department of Chemistry, University of Florida, Gainesville, Florida 32611-7200

Received May 8, 1997. Revised Manuscript Received September 29, 1997[⊗]

Zirconium phosphonate Langmuir−Blodgett (LB) films have been prepared where phenoxy and biphenoxy functional groups are placed in the organic tail at different positions relative to the phosphonate headgroup. The organophosphonic acids 4-octadecyloxyphenylphosphonic acid (P0), 4-(4′-tetradecyloxyphenyl)butylphosphonic acid (P4), 4′-octadecyloxybiphenylphosphonic acid (B0), and 4-(4′-tetradecyloxybiphenyl)butylphosphonic acid (B4) were synthesized for this study. Pressure vs area isotherms of Langmuir monolayers are well-behaved except in the case of B0, where aggregation results in a very rigid monolayer. Using a previously developed three-step deposition procedure, both alternating layer and symmetric bilayer zirconium phosphonate films have been prepared and characterized. A combination of XPS, X-ray diffraction, and ATR-FTIR analyses indicate that organized zirconium phosphonate LB layers are formed in each case. Polarized ATR-FTIR was used to determine the orientation of the different functional groups leading to models for the molecular orientation within the films. In cases where the phenoxy or biphenoxy groups are separated from the phosphonate headgroup, deuteration of the terminal alkyl chain allows for the resolution of the different alkyl segments. Differences in molecular orientations are observed depending on whether the monolayers are deposited on the downstroke (template layer) or on the upstroke (capping layer) of the three-step deposition procedure, and these differences are attributed to the strong zirconium−phosphonate bonding. Subtle orientational differences are also seen for the same capping layers deposited onto different templates. The results show that the zirconium phosphonate LB deposition method may be extended beyond simple alkylphosphonates to organic groups containing aromatic moieties.

Introduction

The Langmuir−Blodgett (LB) technique provides an elegant method for the layer-by-layer deposition of organic films.[1−3] In the LB method, organized monolayers of amphiphilic organic molecules are first prepared at a water surface and then transferred onto a solid support. Organized assemblies of functionalized organic molecules have been prepared in this way for applications that include studies of membrane dynamics,[1] investigations of energy transfer in controlled geometries,[4] and molecular electronics,[5] along with many others.

Recent work[6−12] has shown that it is possible to incorporate known solid-state inorganic layered structures into LB films and to use the inorganic lattice to organize the organic component of the films. LB films of metal salts of octadecylphosphonic acid (OPA) with a variety of divalent metals[7,10,12] and the tetravalent Zr^{4+} [6,8,9,11] have been described. In each case, metal phosphonate layered structures previously known in the solid state were observed in the polar region of head-to-head octadecylphosphonate bilayers. The metal phosphonate bonding can be tuned among known bonding motifs by changing the metal ion, and in turn the packing of the organic groups can be varied. The inorganic lattice can also be used to incorporate new properties into LB films, and we have recently observed magnetic order in the form of canted antiferromag-

* To whom correspondence should be addressed.

[⊗] Abstract published in *Advance ACS Abstracts,* December 1, 1997.

(1) *Langmuir−Blodgett Films*; Roberts, G. G., Ed.; Plenum Press: New York, 1990.
(2) Ulman, A. *An Introduction to Ultrathin Organic Films: From Langmuir−Blodgett to Self-Assembly*; Academic Press: Boston, 1991.
(3) Blodgett, K. B. *J. Am. Chem. Soc.* **1935**, *57*, 1007.
(4) Kuhn, H.; Möbius, D.; Bücher, H. In *Physical Methods of Chemistry*; Weissberger, A., Rossiter, B., Eds.; John Wiley and Sons: New York, 1972; Vol. 1, Part IIIB, pp 577−715.
(5) Bryce, M. R.; Petty, M. C. *Nature* **1995**, *374*, 771−776.
(6) Byrd, H.; Pike, J. K.; Talham, D. R. *Synth. Met.* **1995**, *71*, 1977−1980.
(7) Byrd, H.; Pike, J. K.; Talham, D. R. *J. Am. Chem. Soc.* **1994**, *116*, 7903−7904.
(8) Byrd, H.; Whipps, S.; Pike, J. K.; Ma, J.; Nagler, S. E.; Talham, D. R. *J. Am. Chem. Soc.* **1994**, *116*, 295−301.
(9) Byrd, H.; Pike, J. K.; Talham, D. R. *Chem. Mater.* **1993**, *5*, 709−715.
(10) Seip, C. T.; Byrd, H.; Talham, D. R. *Inorg. Chem.* **1996**, *35*, 3479−3483.
(11) Byrd, H.; Pike, J. K.; Showalter, M. L.; Whipps, S.; Talham, D. R. In *Interfacial Design and Chemical Sensing*; Mallouk, T. E., Harrison, D. J., Eds.; American Chemical Society: Washington, 1994; ACS Symposium Series 561; pp 49−59.
(12) Seip, C. T.; Granroth, G. E.; Meisel, M. W.; Talham, D. R. *J. Am. Chem. Soc.* **1997**, *119*, 7084−7094.

S0897-4756(97)00337-2 CCC: $15.00
Published on Web 01/19/1998

Scheme 1. Alternating Layer and Symmetric Y-type LB Films

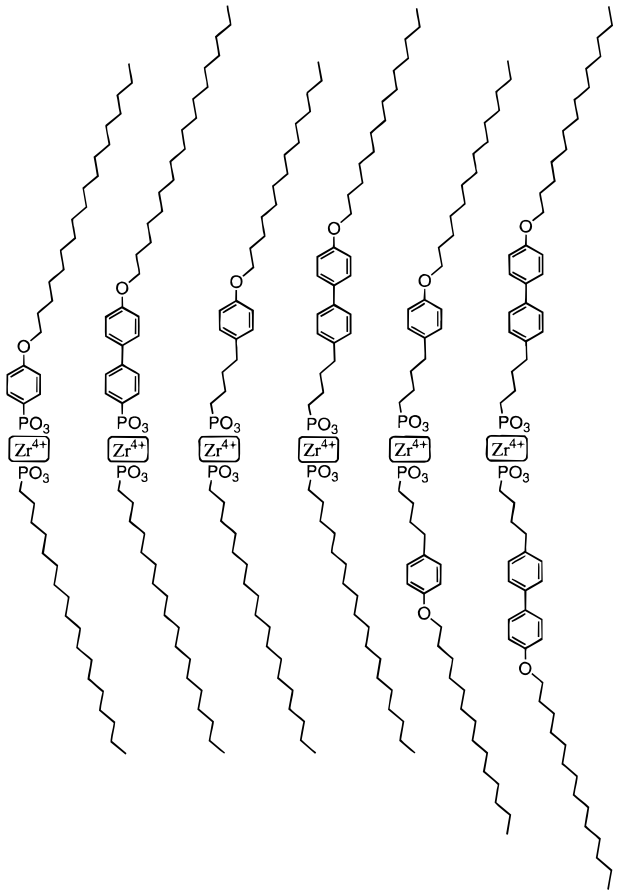

netism in an LB film of manganese octadecylphosphonate.[12] Similarly, layered metal phosphonates have also been used in the construction of self-assembled films[13−15] where, for example, a variety of zirconium phosphonate films have been explored.

The metal phosphonate network provides an opportunity to form mixed organic/inorganic LB films where both components add function to the LB assembly. Since previous metal phosphonate LB films have been formed only with octadecylphosphonic acid, we wish to explore the range of organic functional groups that can be assembled into metal phosphonate LB films. In this article we describe zirconium phosphonate LB films where the organophosphonate contains phenoxy and biphenoxy groups at different positions along the organic tail. The organophosphonic acids (**1**−**6**) used for this study are shown in Scheme 1. When discussing the LB films, we will refer to the molecules using the abbreviations P0, B0, P4, B4, dP4, and dB4, where P and B indicate a phenoxy or a biphenoxy functional group, 0 and 4 refer to the number of carbon atoms separating the aryl group from the phosphonic acid group, and the prefix d indicates that the alkyl tail is perdeuterated. These functionalized phosphonic acids serve as models for determining whether larger organic groups can be organized within the metal phosphonate LB framework. We can also

Scheme 2. Three-Step Procedure for the Deposition of Zirconium Phosphonate Bilayers

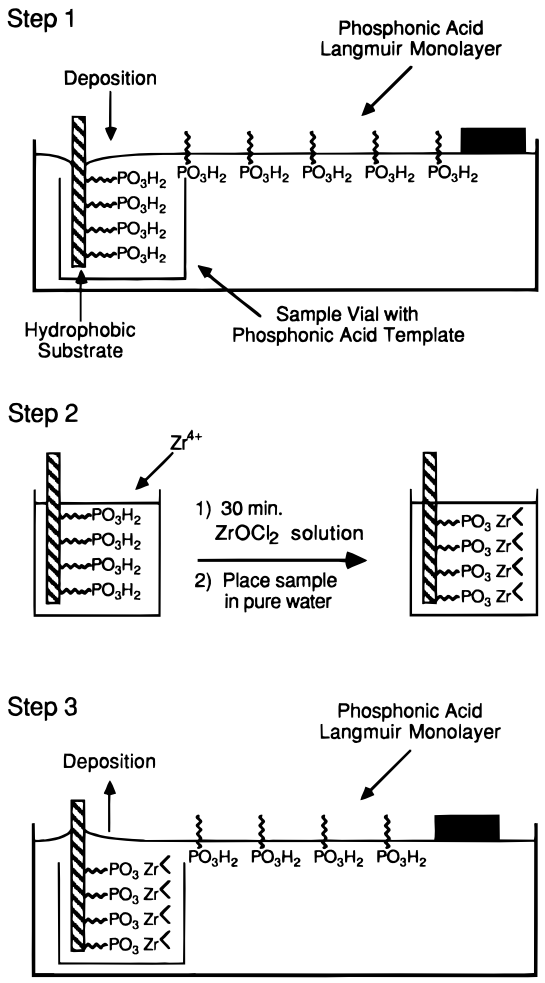

determine how the organization of the films changes as the position of the aryl functional group is varied with respect to the polar phosphonate headgroup.

While the zirconium phosphonate lattice does not add any potentially interesting optical, electronic, or magnetic properties to the organic/inorganic assemblies, the strong oxophilicity of the Zr^{4+} ion brings high inorganic lattice energy to the layered films, making the LB films extremely stable.[8,9,11] In fact, since the zirconium/phosphonate interaction is so strong, the usual LB deposition procedure where metal ions are present in the subphase is not possible because the zirconium ions cross-link the organophosphonate Langmuir monolayers, making the films too rigid to transfer.[9] An alternative stepwise deposition procedure that takes advantage of the strong zirconium phosphonate binding was previously developed for preparing zirconium octadecylphosphonate LB films (Scheme 2).[8,9] This deposition procedure allows for convenient fabrication of symmetric as well as alternating-layer Y-type LB films. In addition, the stepwise procedure permits complete structural characterization of the individual layers deposited on either the downstroke or the upstroke of the deposition cycle.

Each of the alternating layer and symmetric bilayer zirconium phosphonate films that have been prepared and characterized are shown in Scheme 1. Structural characterization of the deposited films includes FTIR,

(13) Cao, G.; Hong, H.-G.; Mallouk, T. E. *Acc. Chem. Res* **1992**, *25*, 420−427.
(14) Katz, H. E. *Chem. Mater.* **1994**, *6*, 2227−2232.
(15) Thompson, M. E. *Chem. Mater.* **1994**, *6*, 1168−1175.

Scheme 3. Synthesis of Phosphonic Acids

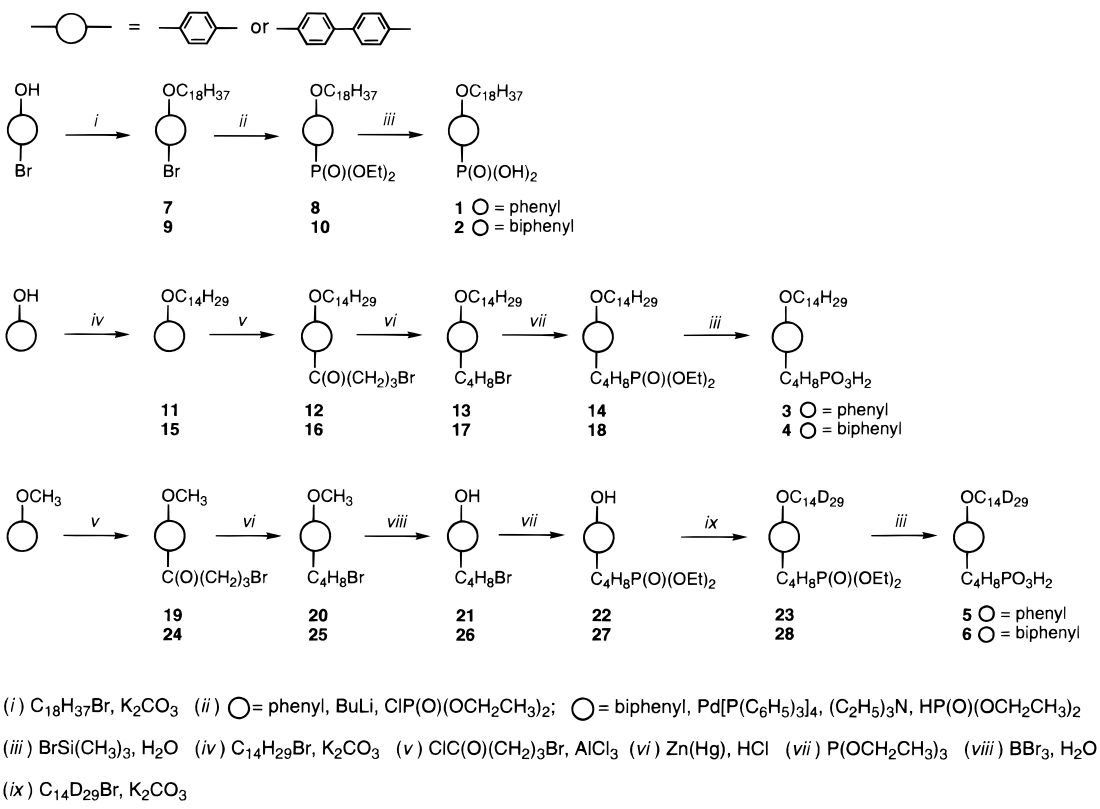

(*i*) $C_{18}H_{37}Br$, K_2CO_3 (*ii*) = phenyl, BuLi, $ClP(O)(OCH_2CH_3)_2$; = biphenyl, $Pd[P(C_6H_5)_3]_4$, $(C_2H_5)_3N$, $HP(O)(OCH_2CH_3)_2$

(*iii*) $BrSi(CH_3)_3$, H_2O (*iv*) $C_{14}H_{29}Br$, K_2CO_3 (*v*) $ClC(O)(CH_2)_3Br$, $AlCl_3$ (*vi*) Zn(Hg), HCl (*vii*) $P(OCH_2CH_3)_3$ (*viii*) BBr_3, H_2O

(*ix*) $C_{14}D_{29}Br$, K_2CO_3

XPS, and X-ray diffraction studies. The results show that phenoxy and biphenoxy groups can be incorporated into zirconium phosphonate LB films. In general, the functionalized molecules behave rather similarly with the exception of B0, which strongly aggregates, even at the water surface. Because of the nature of the stepwise deposition procedure and the strong zirconium phosphonate bonding, subtle differences in the organization of molecules within a layer can be observed that depend on whether the layer is deposited on the downstroke or on the upstroke.

Experimental Section

Materials. Octadecylphosphonic acid (OPA), $C_{18}H_{39}O_3P$, was obtained from Alfa Aesar (Ward Hill, MA) and used as supplied. Zirconyl chloride, 98%, was purchased from Aldrich (Milwaukee, WI). HPLC grade chloroform, stabilized with amylene, was used as received from Acros (Pittsburgh, PA). Octadecyltrichlorosilane (OTS), $C_{18}H_{37}SiCl_3$, 95%, was purchased from Aldrich and stored under nitrogen.

Synthesis. 4-Octadecyloxyphenylphosphonic acid (P0, **1**), 4-octadecyloxybiphenylphosphonic acid (B0, **2**), 4-(4′-tetradecyloxyphenyl)butylphosphonic acid (P4, **3**), 4-(4′-tetradecyloxybiphenyl)butylphosphonic acid (B4, **4**), 4-(4′-d_{29}-tetradecyloxyphenyl)butylphosphonic acid (dP4, **5**), and 4-(4′-d_{29}-*p*-tetradecyloxybiphenyl)butylphosphonic acid (dB4, **6**) were prepared as shown in Scheme 3. Full synthetic details for each compound and intermediate are included in the Supporting Information.

Substrate Preparation. Single-crystal (100) silicon wafers, purchased from Semiconductor Processing Co. (Boston, MA), were used as deposition substrates for X-ray photoelectron spectroscopy (XPS). X-ray diffraction samples were prepared on petrographic slides that were purchased from Buehler Ltd (Lake Bluff, IL). Silicon and germanium attenuated-total-reflectance (ATR) crystals, 50 mm × 10 mm × 3 mm with 45° faces, purchased from Wilmad Glass (Buena, NJ), were used as substrates for FTIR-ATR experiments. The

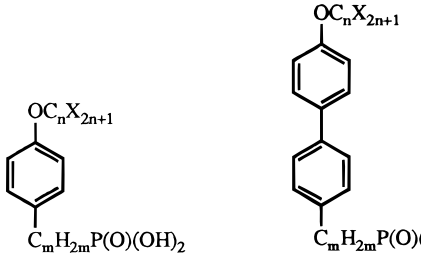

1 (P0) X=H, n=18, m=0
3 (P4) X=H, n=14, m=4
5 (dP4) X=D, n=14, m=4

2 (B0) X=H, n=18, m=0
4 (B4) X=H, n=14, m=4
6 (dB4) X=D, n=14, m=4

silicon and glass substrates were cleaned using the RCA[16] procedure and dried under nitrogen. All substrate surfaces were made hydrophobic by deposition of a monolayer of OTS.[17,18]

Instrumentation. The Langmuir−Blodgett (LB) experiments were performed using KSV Instruments (Stratford, CT) 5000 and 3000 systems with homemade Teflon-coated troughs modified to operate with double barriers. Pressure versus area ($\pi-A$) isotherms were recorded on either of these systems with surface areas of 794 cm^2 (12.8 cm × 67 cm) and 960 cm^2 (12.8 cm × 75 cm) for the 3000 and 5000 instruments, respectively. A Barnstead NANOpure (Boston, MA) purification system produced water with a resistivity of 17.5−18 MΩ cm for all experiments. Surface pressure was measured with a platinum Wilhelmy plate suspended from a KSV microbalance. For studies of LB film behavior as a function of subphase pH, the appropriate amount of 0.012 M HCl or 0.01 M KOH was added to 2 L of pure water to obtain values of 3−8. The pH of the subphase was stable over the time scale of the experiments.

Infrared spectra were recorded on a Mattson Instruments (Madison, WI) Research Series-1 FTIR spectrometer with

(16) Kern, W. *J. Electrochem. Soc.* **1990**, *137*, 1887−1892.
(17) Maoz, R.; Sagiv, J. *J. Colloid Interface Sci.* **1984**, *100*, 465−496.
(18) Netzer, L.; Sagiv, J. *J. Am. Chem. Soc.* **1983**, *105*, 674−676.

either a mercury−cadmium−telluride (MCT) or deuterated triglycine sulfate (DTGS) detector. LB films were deposited onto OTS-coated Si or Ge ATR parallelograms, and a Harrick (Ossing, NY) TMP stage was used for the ATR experiments. Polarized FTIR-ATR spectra were taken with s- and p-polarized light. All FTIR-ATR spectra consist of 1000 scans at 4 cm^{-1} resolution and were referenced to the appropriate background.

X-ray diffraction patterns were obtained with a Phillips APD 3720 X-ray powder diffractometer with the Cu Kα line, λ = 1.54 Å as the source. XPS was performed on a Perkin-Elmer (Eden Prairie, MN) PHI 5000 series spectrometer. All spectra were taken using the Mg Kα line at 1253.6 eV. The spectrometer has a typical resolution of 2.0 eV, with anode voltage and power settings of 15 kV and 300 W, respectively. Typical operating pressure was 5×10^{-9} atm. All XPS spectra were recorded with a 45° takeoff angle. Survey scans consisted of five scans performed with 0.5 eV/step, 20 ms/step, and a pass energy of 89.45 eV, and multiplex scans consisted of 80 scans/region taken in 10 sweeps/cycle operating at 0.1 eV/step, 50 ms/step, and a pass energy of 37.75 eV.

Results and Discussion

Synthesis. Compounds **1**−**6** were synthesized as outlined in Scheme 3. The methods employed to form P−C bonds are well established.[19−24] In the case of **1**, metal−halogen exchange was followed by reaction with the appropriate phosphorus electrophile, a procedure outlined by Katz et al.[20,21] for the synthesis of aromatic phosphonate compounds. The reaction proceeded in only modest yields as it appears that the long alkyl chains necessary for forming stable Langmuir monolayers hinder the normally high yields of this method. For **2**, better yields were realized using the palladium-catalyzed phosphorylation reaction developed by Hirao et al.[23,24] The Arbuzov reaction[22] furnished the aliphatic phosphonate esters in a straightforward manner. Dealkylation with $(CH_3)_3SiBr$[20,21] proved a facile method for the convenient hydrolysis of phosphonate esters, yielding the final, analytically pure product in each case.

Langmuir Monolayers. Compounds P0, P4, B0, and B4 were characterized at the air/water interface. Figure 1 shows pressure vs area isotherms of each compound during compression on a pure water subphase at pH 5.5. While Langmuir monolayers of P0, P4, and B4 give reasonable pressure vs area isotherms, B0 behaves very differently.

Isotherms of P4 and B4 are similar with nearly parallel slopes in well-defined liquid compressed regions and with mean molecular areas (MMA) at collapse of 24.8 and 24.2 ± 0.3 $Å^2$, respectively. We define film collapse as the point on the compression curve where deviations from the linear slope of the liquid compressed region are first observed. Areas at collapse for P4 and B4 are greater than the 20 $Å^2$ MMA at collapse reported for OPA on a water subphase.[25] A MMA between 24 and 25 $Å^2$ corresponds nicely to the cross-sectional areas of phenoxy or biphenoxy units oriented with their long axes tilted slightly from the normal to the surface[26] and indicates that interactions between the aromatic groups are responsible for determining the areas per molecule within the Langmuir monolayers.

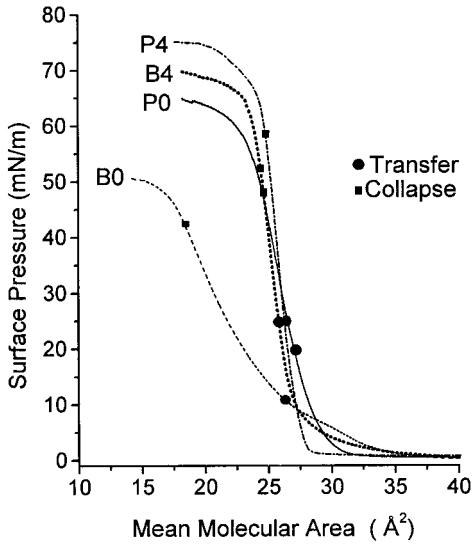

Figure 1. Pressure vs area isotherms of P4, B4, P0, and B0 on a pure water subphase at pH 5.5. Spreading solutions used in these experiments had concentrations between 0.2 and 0.4 mg/mL in $CHCl_3$ for P4 (dP4), in 10% EtOH/$CHCl_3$ for P0, B4 (dB4), and in 30% EtOH/$CHCl_3$ for B0. Between 100 and 400 μL of solution was spread on the water surface for each experiment, and compression was performed with a linear compression rate of 1 mN/(m min) and with maximum barrier speeds of 1 mm/min. Pressures and areas at which the films are transferred to substrates and at which the films collapse are highlighted with circles and squares, respectively.

The isotherm of P0 shows a MMA at collapse of 24.3 $Å^2$, which is similar to the areas observed for P4 and B4 and reflects the presence of the phenyl group in this molecule. However, the slope of the liquid compressed region is not as steep as those observed in the isotherms of P4 and B4. The more shallow slope results from increased rigidity of this film. Unlike P4 and B4, where the four-carbon tether between the aromatic and phosphonate groups provides flexibility, the phenyl group in P0 is incorporated into a position adjacent to the headgroup. The phenylphosphonate groups appear to aggregate at the water surface, resulting in a more rigid film. The rigidity of the film is also apparent during film deposition, as discussed below. This situation is far more pronounced in the case of B0. In the isotherm of B0, the surface pressure first begins to rise at about the same point as P0 (MMA between 35 and 40 $Å^2$), but as the isotherm progresses an unreasonably low MMA of 17 ± 0.5 $Å^2$ is observed for the collapse point. In this case the rigidity of the film, resulting from aggregation of the molecules, precludes accurate measurement of the surface pressure using the Wilhelmy plate method. In some cases, the Wilhelmy plate can be observed to drift. On the basis of the pressure vs area isotherm alone, we cannot determine the exact state of the B0 monolayer at the air/water interface. However, from studies of

(19) *Organic Phosphorus Compounds*; Kosolapoff, G. M., Maier, L., Eds.; Wiley-Interscience: New York, 1976; Vol. 7.
(20) Katz, H. E.; Bent, S. F.; Wilson, W. L.; Schilling, M. L.; Ungashe, S. B. *J. Am. Chem. Soc.* **1994**, *116*, 6631−6635.
(21) Katz, H. E.; Wilson, W. L.; Scheller, G. *J. Am. Chem. Soc.* **1994**, *116*, 6636−6640.
(22) Bhattacharya, A. K.; Thyagarajan, G. *Chem. Rev. (Washington, D.C.)* **1981**, *81*, 415−430.
(23) Hirao, T.; Masunaga, T.; Ohshiro, Y.; Agawa, T. *Synthesis* **1981**, 56−57.
(24) Hirao, T.; Masunaga, T.; Yamada, N.; Ohshiro, Y.; Agawa, T. *Bull. Chem. Soc. Jpn.* **1982**, *55*, 909−913.
(25) Ries Jr., H. E.; Cook, H. D. *J. Colloid Sci.* **1954**, *9*, 535−546.
(26) Tillman, N.; Ulman, A.; Schildkraut, J. S.; Penner, T. L. *J. Am. Chem. Soc.* **1988**, *110*, 6136−6144.

transferred films, which are described below, we believe that a close-packed Langmuir monolayer is present at a reasonable MMA, such as those observed for P0, P4, and B4.

Studies of the pressure vs area isotherms for each phosphonic acid as a function of subphase pH show that at higher pH, typically greater than 7, the slopes of the liquid compressed region become more shallow. This effect is most pronounced in the isotherms of B0 and B4, whereas pH-dependent effects are more subtle for P0 and P4. Deuteration of the 14-carbon segment in P4 and B4 does not affect the behavior of monolayer isotherms.

Deposition Procedure. A three-step deposition procedure was utilized for preparing the zirconium organophosphonate films described in this paper. This stepwise deposition method was developed previously for preparing LB bilayers of zirconium octadecylphosphonate.[8,9] As illustrated in Scheme 2, the first step involves creation of an LB monolayer by dipping an OTS-coated substrate down through a compressed monolayer on a pure water subphase into a vial sitting in the dipping well of the trough. We refer to this layer deposited on the downstroke as the "template" layer. The Langmuir monolayer is then decompressed, and the vial containing the template-coated substrate is removed from the trough. In the second step $ZrOCl_2$ is added to the vial containing the substrate to bring the Zr^{4+} ion concentration in the vial to 5 mM. These conditions permit zirconium binding to the phosphonic acid, and after 20 min[27] the substrate containing the zirconated template layer is removed from the solution and rinsed with pure water. The zirconated template is a stable structure, and information regarding its organization and structure can be obtained. Without zirconation, however, the template monolayer is metastable, and characterization cannot be performed. This substrate is next returned to the trough, which is filled with a fresh subphase of pure water. For the final step, a new Langmuir monolayer is compressed at the air−water interface, and a new LB monolayer is deposited as the substrate is drawn upward through the film. The layer deposited onto the zirconated template is referred to as the "capping" layer. This capping layer can also be individually characterized. Multilayer assemblies can be prepared by repeating this three-step procedure.

By exploiting the versatility of this deposition procedure, particularly the ability to prepare bilayers where the template layer is different from the capping layer, we are able to generate a variety of Y-type zirconium organophosphonate LB films. Table 1 lists the deposition conditions used to prepare the films shown in Scheme 1. Transfer ratios for all the films were 1.1 ± 0.15, with the values uncorrected for any creep of the films. For depositions, all LB films were compressed with a linear compression rate of 8 mN/(m min) and with maximum barrier speeds of 20 mm/min. Typically 100−350 μL of a 0.3 mg/mL solution was spread on the water surface for each experiment. The compressed monolayer films were allowed to stabilize 5−20 min before they were transferred to the substrate.

(27) XPS determination of Zr:P ratios were performed to determine the optimum time necessary for zirconium binding.

Table 1. Deposition Conditions[a] for the Template[b] and Capping[c] LB Monolayers

	target pressure[d] (mN/m)	film aging time (min)	dipping speeds (mm/min)
OPA	20	5	8
P4 (dP4)	25	10	3
B4 (dB4)	25	5	2
P0[e]	20	15	1
B0[e]	12	20	1

[a] For all depositions, films were compressed with a linear compression rate of 8mN/(m min) and with barrier speeds of 20 mm/min. [b] Template layers were initially transferred onto an OTS-coated substrate. [c] Depostion conditions for the capping layers are the same regardless of the identity of the zirconated LB template monolayer. [d] Target pressures correspond to a MMA of 24 Å^2 for OPA and a MMA of 27 ± 1 Å^2 for all other materials. [e] PO and BO can be transferred only as capping monolayers.

In addition to using OPA as a template layer,[8,9] template layers can be formed with P4 and B4. However, despite several attempts under various conditions, quality template layers of P0 and B0 monolayers could not be deposited. This difference in behavior indicates that the position of the aryl group along the aliphatic chain plays a significant role in the processability of these Langmuir monolayers. Differences between the molecules with the four-carbon alkyl tether (P4, B4) and the arylphosphonates (P0, B0) were also seen in the pressure vs area isotherms, where it was observed that the P0 and B0 molecules tended to aggregate on the water surface. Aggregation of the organic functionalities when they are adjacent to the phosphonate headgroups not only affects the behavior of the film on the surface of the water but also appears to cause difficulties in the transfer of these films. In contrast, the four-carbon tether in P4 and in B4 separates the aryl group from the phosphonate headgroup leading to a less rigid, more processible film. The four-carbon tether allows the two sections of the molecule to organize relatively independently of one another, separating the polar headgroup from the constraints of the packing of the aromatic groups. This flexibility of the headgroup appears to lead to well-behaved isotherms and to successful downstroke depositions of P4 and B4 monolayers.

Although quality template layers of P0 and B0 could not be formed, these films, along with P4 and B4, were successfully deposited as capping layers. Here, the position of the organic moiety along the alkyl chain has less influence on the film processability. Transfer of the capping layers is aided by the affinity of the phosphonate groups for the zirconium ions on the substrate. The strength of this interaction is the driving force for the deposition of the capping monolayers, and it overcomes any rigidity or disorganization of the monolayer on the water surface. Alternating layer films were formed by transferring P0, P4, B0, and B4 onto OPA template layers. In addition, symmetric bilayer films of P4 and B4 were prepared by transferring P4 and B4 capping layers onto the appropriate template layers.

XPS Analyses. XPS analyses show that C, O, P, and Zr are the only elements present in each film. Signals due to Si also appear from the silicon wafer substrates onto which the films are deposited. The relative percentages of Zr and P observed for each sample are listed in Table 2. The percentages listed in Table 2 have not

Table 2. Interlayer Spacings[a] and Relative Intensities[b] of the Zirconium and Phosphorus XPS Signals[c] of the Zirconated Template LB Monolayer and LB Bilayer Films

	Zr (±3%)	P (±3%)	*d*-spacing, experimental (± 2Å)	*d*-spacing, calculated[d] (± 2Å)
zirconated templates				
OPA−Zr	48	52		
P4−Zr	48	52		
B4−Zr	46	54		
bilayer samples				
OPA−Zr−P0	31	69	53	51
OPA−Zr−P4	36	64	52	51−53
OPA−Zr−BO	34	66	57	58
OPA−Zr−B4	32	68	54	54−56
P4−Zr−P4	32	68	56	52−55
B4−Zr−B4	32	68	62	61−63

[a] X-ray samples consisted of 10 bilayers of deposited films. [b] Relative intensity percentages for zirconium and phosphorus were calculated by integrating the areas of the corresponding peaks after correcting for the instrument and atomic sensitivity factors. [c] The Zr 3d and P 2p peaks were used for this calculation. [d] Calculated *d*-spacings were determined as described in the text. For those films having a four-carbon tether, a range is reported since the orientation of this four-carbon chain is not known. The smaller value is obtained when the four-carbon chain is allowed to tilt at the same angle as the 14-carbon chain, while the larger value results if the 4-carbon chain is oriented perpendicular to the surface. A van der Waals distance of 5 Å was used for all calculations.

been corrected for differences in photoelectron escape depths.[28−32] Because the photoelectron energies of the Zr 3d (185.9 eV, 183.6 eV) and P 2p (134.3 eV) are similar and the Zr and P atoms are at nearly the same depth in the films, corrections for photoelectron escape depths are less than 1% of the observed intensities. Within the uncertainties of the XPS method (±3%), the observed Zr:P ratio in the zirconated templates of OPA, P4, and B4 is 1:1, indicating that after zirconation, one zirconium ion is bound for each phosphonate group in the template layer. For the bilayer samples, Zr:P ratios are all near 1:2, indicating complete transfer of the capping layer. The 1:2 ratio is consistent with the Zr:P ratios and the ionic charges present in solid-state zirconium organophosphonates.

In bilayer samples where OPA is the template layer there is a mismatch between the MMA of the molecules in the template and capping layers because of the larger aryl group in the organic tails of the capping layer. The MMA of OPA in a monolayer film is 24 Å^2, while the MMA in transferred monolayers of P0, B0, P4, and B4 is 27 ± 1 Å^2 (note that the MMA during transfer of Langmuir monolayers is greater than the MMA at the collapse point, which was referred to earlier during the discussion of the pressure vs area isotherms). The incommensurate spacing between the capping layer and the zirconated template, resulting from the different sizes of the molecules, leads to expected values of 34.6% Zr and 65.4% P or a Zr:P ratio of 1:1.9 for the alternate layer films. The observed XPS ratios are consistent with the expected percentages, although we cannot actually observe that the phosphonate coverages are incommensurate because of the magnitude of the uncertainty in elemental composition when determined by XPS.

X-ray Diffraction. The layered nature of the films was established by X-ray diffraction. Interlayer spacings were determined from samples containing 10 bilayers of deposited materials. On average three or four orders of (00*l*) reflections were observed for each sample, and the interlayer spacings for each film, determined from the (00*l*) peaks, are reported in Table 2. In general, layers containing the larger biphenyl group, B0 or B4, are thicker than the corresponding P0 or P4 layers, as expected assuming the molecules are oriented in a similar fashion. Interestingly, even though the P0, P4 and B0, B4 pairs have the same size (i.e., P0 contains the same number of methylene groups as P4 and should be the same size), the OPA−Zr−P0 and OPA−Zr−B0 layers are slightly thicker than the corresponding OPA−Zr−P4 and OPA−Zr−B4 films. The different layer thicknesses reflect different modes of molecular packing. The arrangement of molecules within the transferred layers is discussed further below after considering the results of the FTIR analyses.

Infrared Analyses. To investigate the organization of the organophosphonate groups in samples shown in Scheme 1, ATR-FTIR[33−35] spectra of the zirconated template monolayers and of the subsequent capping monolayers were obtained. For these studies, ATR-FTIR scans were acquired after the second and final steps of the deposition procedure. Ratioing to the appropriate background produced spectra of the individual template monolayers and capping monolayers. Information regarding the arrangement of the aryl moieties was obtained through analysis of spectra of multilayer samples.

Template Layers. We have previously shown that template layers of OPA display the organized structure necessary for constructing stable, well-organized multilayer films.[8,9,11] Successful transfers of P4 and B4 on the deposition downstroke result in new template layers that may be compared with the template layer of OPA. Figure 2 compares ATR-FTIR spectra from 2700 to 3100 cm^{-1} of zirconated template monolayers of OPA, P4, and B4. In all spectra three C−H stretching bands are resolved corresponding to the asymmetric methyl stretch ($\nu_a(CH_3)$) at 2953 cm^{-1}, the asymmetric methylene stretch ($\nu_a(CH_2)$) at 2918 cm^{-1}, and the symmetric methylene stretch ($\nu_s(CH_2)$) at 2850 cm^{-1}. These modes are commonly used to assess the conformational order and the extent of organization of the aliphatic chains. In particular, the frequency of the asymmetric methylene stretch reflects the conformational order of the alkyl chains,[33,35] and its fwhm is a measure of the degree to which the alkyl chains are close-packed.[34,35] For an all-trans conformation of the alkyl chains in a crystalline

(28) Brundle, C. R.; Hopster, H.; Swalen, J. D. *J. Chem. Phys.* **1979**, *70*, 5190−5196.
(29) Seah, M. P.; Dench, W. A. *Surf. Interface Anal.* **1979**, *1*, 1−11.
(30) Akhter, S.; Lee, H.; Hong, H.-G.; Mallouk, T. E.; White, J. M. *J. Vac. Sci. Technol.* **1989**, *7*, 1608−1613.
(31) Laibinis, P. E.; Bain, C. D.; Whitesides, G. M. *J. Phys. Chem.* **1991**, *95*, 7017−7021.
(32) Sastry, M.; Ganguly, P.; Badrinarayanan, S.; Mandale, A. B.; Sainkar, S. R.; Paranjape, D. V.; Patil, K. R.; Chaudhary, S. K. *J. Chem. Phys.* **1991**, *95*, 8631−8635.
(33) Porter, M. D.; Bright, T. B.; Allara, D. L.; Chidsey, C. E. D. *J. Am. Chem. Soc.* **1987**, *109*, 3559−3568.
(34) Wood, K. A.; Snyder, R. G.; Strauss, H. L. *J. Chem. Phys.* **1989**, *91*, 5255−5267.
(35) Maoz, R.; Sagiv, J. *J. Colloid Interface Sci.* **1984**, *100*, 465−496.

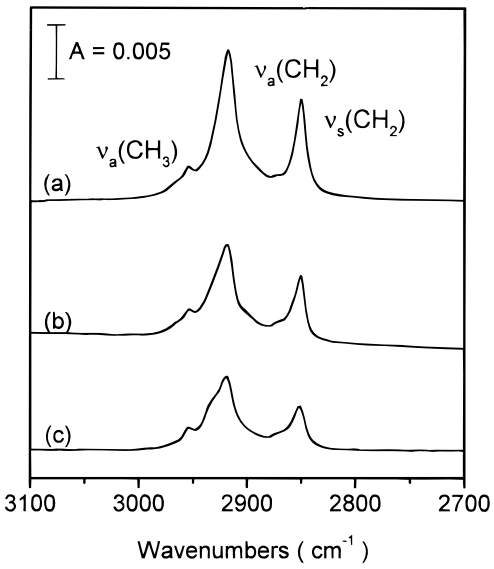

Figure 2. ATR-FTIR spectra of zirconated monolayer templates of (a) OPA, (b) P4, and (c) B4. Band assignments are discussed in the text.

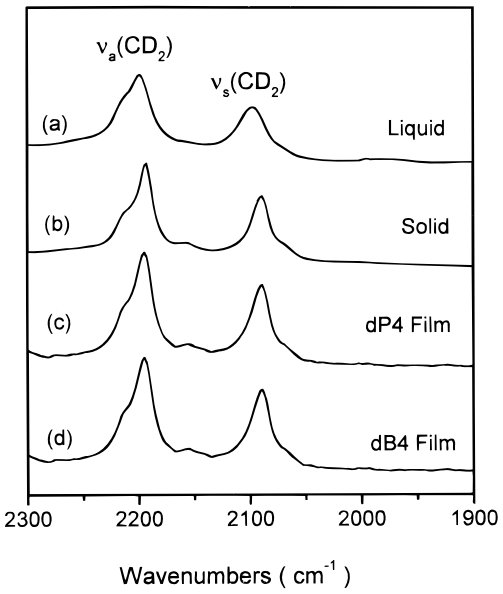

Figure 3. FTIR spectra of (a) a $CHCl_3$ solution of dP4 and (b) a KBr pellet of dP4 and ATR-FTIR spectra of (c) dP4 as a zirconated template layer and (d) dB4 as a zirconated template layer. Band assignments are discussed in the text. The spectra are scaled in intensity for comparison of band shapes and frequencies.

solid of OPA, $\nu_a(CH_2)$ occurs near 2918 cm^{-1}, and this value increases in energy to 2926 cm^{-1} in a liquidlike assembly where the alkyl chains possess a large number of gauche bonds.[26] The fwhm is a measure of the orientational order in the film, and typical values of 16 cm^{-1} have been observed for a close-packed monolayer of OTS,[26] whereas a randomly oriented film can result in a fwhm for $\nu_a(CH_2)$ of greater than 35 cm^{-1}.[9] In the spectra shown in Figure 2, a peak position of 2918 cm^{-1} for the asymmetric methylene vibration indicates that all three template layers possess alkyl chains arranged in an all-trans conformation. For the OPA template, where the alkyl chains have previously been shown to be close-packed, the fwhm of $\nu_a(CH_2)$ is 20 cm^{-1}.[9] In contrast, the fwhm values for P4 and for B4 are 27 and 29 cm^{-1}, respectively. The bands are broadened in the P4 and B4 monolayer spectra because they contain contributions from both the 14-carbon and 4-carbon segments.

To differentiate the signals originating from the 14-carbon and 4-carbon segments in P4 and B4, ATR-FTIR studies of dP4 and dB4, where the 14-carbon chain was perdeuterated, were performed. To determine how the C−D stretching modes shift as a function of the state of the molecule, spectra were first taken of the deuterated samples in $CHCl_3$ solutions and as solids (KBr pellet). Spectra showing the C−D stretches of dP4 are compared in Figure 3. The solution samples of both dP4 and dB4 have the asymmetric methylene stretch ($\nu_a(CD_2)$) at 2198 cm^{-1} and the symmetric methylene stretch ($\nu_s(CD_2)$) at 2096 cm^{-1}. This is in contrast to the $\nu_a(CD_2)$ and $\nu_s(CD_2)$ positions in the spectra of the solids at 2193 and 2089 cm^{-1}, respectively. The asymmetric CD_2 stretch also has a large fwhm of 35 cm^{-1} in the solution spectra as opposed to the 20 cm^{-1} value for those of the solids. Figure 3 also shows the C−D stretch region of template monolayers of dP4 and dB4 where for both the $\nu_a(CD_2)$ and $\nu_s(CD_2)$ bands appear at 2195 and 2090 cm^{-1}, respectively. The bands are narrow, with a fwhm of 20 cm^{-1}, and appear essentially identical with the solid-state KBr spectra of dP4 shown in Figure 3. This result indicates that the 14-carbon alkyl chains in the templates of dP4 and dB4 are well-organized and are arranged in an all-trans conformation, suggesting that the broadened $\nu_a(CH_2)$ stretch observed in the spectra of the nondeuterated P4 and B4 template layers (Figure 2) does not result from any disorder in the 14-carbon segment.

Inspection of the C−H modes resulting from the four-carbon segment in monolayer spectra of the dP4 and dB4 templates reveals that the spectra closely resemble the C−H stretch modes observed in a solid-state spectrum of butylphosphonic acid, where individual CH_2 units can be distinguished. The four-carbon segment, therefore, is responsible for the broad C−H stretch modes seen in undeuterated templates of P4 and B4. Although there is a resemblance to the KBr spectrum of butylphosphonic acid, we cannot determine how the four-carbon chains in templates of P4 and B4 are organized.

The tilt angles of the alkyl chains with respect to the surface normal in the template layers of dP4 and dB4, as well as in OPA, were determined from polarized ATR-FTIR experiments. Detailed accounts of the procedure have been included in publications of other researchers.[26,36−38] From ratios of the absorbance intensity of a given IR mode with light polarized parallel and perpendicular to the film surface, a dichroic ratio, defined as

$$D = (A_x + A_z)/A_y \quad (1)$$

where $(A_x + A_z)$ is the absorbance with p-polarized light and A_y is the absorbance with s-polarized light, can be calculated. For the methylene vibrations, the CH_2 dipole moment is oriented 90° with respect to the alkyl

(36) Haller, G. L.; Rice, R. W. *J. Phys. Chem.* **1970**, *74*, 4386-4393.
(37) Cammarata, V.; Atanasoska, L.; Miller, L. L.; Kolaskie, C. J.; Stallman, B. J. *Langmuir* **1992**, *8*, 876−886.
(38) Jang, W.-H.; Miller, J. D. *J. Phys. Chem.* **1995**, *99*, 10272−10279.

Table 3. Dichroic Ratios,[a] *D*, of IR Modes and the Corresponding Molecular Axis[b] Tilt Angles for Zirconated Template Layers

template monolayer	mode	frequency (cm^{-1})	dichroic ratio *D*	tilt angle (deg)
OPA	$\nu_a(CH_2)$	2918	1.04 ± 0.02	30 ± 2
	$\nu_s(CH_2)$	2850	1.04 ± 0.01	30 ± 1
dP4	$\nu_a(CD_2)$	2195	NA[c]	NA[c]
	$\nu_s(CD_2)$	2090	1.28 ± 0.03	46 ± 2
	C=C (8a)	1612	NA[d]	NA[d]
	C=C (19a)	1514	3.4 ± 0.1	20 ± 1[e]
dB4	$\nu_a(CD_2)$	2195	NA[c]	NA[c]
	$\nu_s(CD_2)$	2090	1.25 ± 0.2	44 ± 1
	C=C (8a)	1608	3.4 ± 0.2	20 ± 1[e]
	C=C (19a)	1502	3.8 ± 0.2	19 ± 1[e]

[a] Dichroic ratio, *D*, is defined as $(A_x + A_z)/(A_y)$. [b] Molecular axes are defined along the C1−C4 axis for the phenyl and biphenyl moieties and at 90° to the methylene C−H bonds for the alkyl chains. [c] Tilt angles for the perdeuterated 14-carbon chains were calculated from the symmetric methylene stretch only. [d] Only mode 19a was used to determine the tilt of the phenyl ring. [e] Tilt angles for the aryl groups are averaged over the template and capping layers for the symmetric bilayer films.

chain axis. By taking the ratio of the absorbance intensities of $\nu_a(CH_2)$ and $\nu_s(CH_2)$ with p-polarized light to the intensities with s-polarized light and by noting the relationship between the CH_2 dipole moment and the molecular axis, we were able to determine the angle that the alkyl chains make with respect to the surface normal. Measured dichroic ratios and calculated tilt angles for the 18-carbon chains in OPA and for the 14-carbon chains in dP4 and dB4 templates are given in Table 3. On average, the tilt angle for the 18-carbon segment in the zirconated OPA template is 30°, which correlates well with the tilt required to achieve close-packing of the alkyl chains given the constraints of the PO_3^{2-} headgroup (24 $Å^2$ MMA at deposition opposed to 20 $Å^2$ for the cross-sectional area of the all-trans alkyl chain). For the templates of dP4 and dB4, the tilt angles of the 14-carbon segments are 46° and 44°, respectively. The larger alkyl chain tilt angles in dP4 and dB4 relative to the OPA template arise from a greater spacing between molecules because of the larger MMA (27 $Å^2$ at transfer) imposed by the aryl groups. The larger distance between molecules requires the chains to tilt more to maximize van der Waals interactions. Because of the nature of the IR signals for the four-carbon segments in the dP4 and dB4 templates, an analysis of their molecular axis tilt angles is not meaningful.

Capping Layers. *P0 and B0 on an OPA Template.* Although quality template monolayers of P0 and B0 could not be transferred, monolayer films of these materials were successfully transferred as capping layers onto zirconated OPA templates. The organization of the alkyl chains and aryl groups in these capping monolayers was determined from nonpolarized and polarized IR data. Figure 4 shows nonpolarized ATR-FTIR spectra of capping monolayers of P0 and B0 as deposited onto zirconated OPA templates. In these spectra the asymmetric methylene vibration, $\nu_a(CH_2)$, occurs at 2918 cm^{-1}, indicating that the 18-carbon alkyl chains in both arylphosphonates are arranged in an all-trans conformation. The fwhm values of the asymmetric methylene vibrations in the spectra of P0 and B0 are 20 and 16 cm^{-1}, respectively, indicating that the alkyl chains are close-packed.

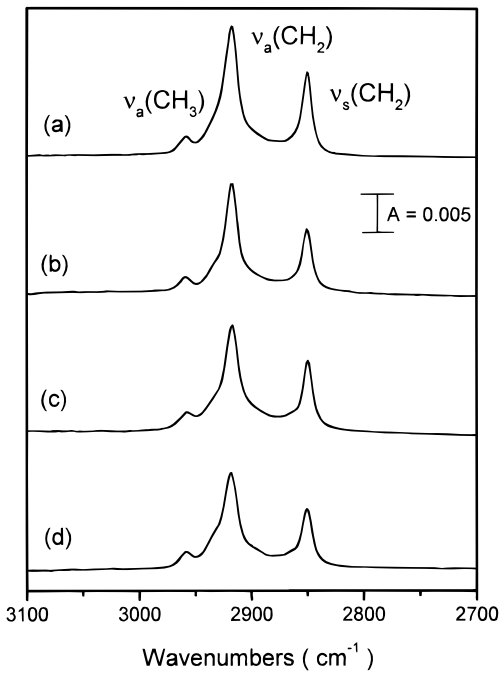

Figure 4. ATR-FTIR spectra of capping monolayers of (a) P0 on OPA, (b) B0 on OPA, (c) P4 on OPA, and (d) B4 on OPA. The capping layers are referenced to the OPA zirconated templates. Band assignments are discussed in the text.

On the basis of the pressure vs area isotherms shown in Figure 1, it was not clear if B0 formed a stable Langmuir monolayer. Analysis of the transferred film, however, indicates that it does. From Figure 4 it can be seen that the intensities of the IR bands for the capping layer of B0 are similar to those of the other capping layers. Coupled with the XPS results that show that a single layer of the phosphonate group is deposited and the X-ray diffraction showing the layered structure of the alternating-layer films, it is clear that B0 transfers as an organized LB monolayer. The Langmuir monolayer of B0 at the air/water interface is too rigid to behave ideally, but it can be transferred onto the zirconated OPA template layers.

The tilt angle of the alkyl chain axis in capping monolayers of P0 and B0 was determined from polarized ATR-FTIR experiments. Dichroic ratios for the $\nu_a(CH_2)$ and $\nu_s(CH_2)$ bands in each film and calculated tilt angles for the alkyl chain molecular axes are reported in Table 4. The measured dichroic ratios, determined from both the asymmetric and symmetric methylene vibrations, indicate that in B0 the alkyl chains tilt an average of 20.5° with respect to the surface normal, whereas in P0 this value is 36°. The 36° alkyl chain tilt in P0 is similar to the large tilt angles seen for the alkyl chains in template layers of P4 and B4 (46° and 44°, respectively) where the MMA is determined by the size of the aryl groups and where the alkyl chains must tilt to maximize van der Waals interactions. The 20.5° tilt angle average observed for the B0 layer appears anomalous and suggests that the mode of intermolecular interaction is different in the B0 film than in the other monolayer template and capping layers. The relationship between the tilt angles of the alkyl chain axis and the aryl moiety with be discussed further below after all of the IR data have been presented.

Table 4. Dichroic Ratios,[a] *D*, of IR Modes and Corresponding Molecular Axis[b] Tilt Angles for Capping Layers Deposited onto Zirconated OPA Templates

capping monolayer (on OPA)	mode	freq (cm^{-1})	dichroic ratio *D*	tilt angle (deg)
P0	$\nu_a(CH_2)$	2918	1.09 ± 0.02	35 ± 2
	$\nu_s(CH_2)$	2850	1.12 ± 0.02	37 ± 2
	C═C (8a)	1603	2.9 ± 0.1	22 ± 1
	C═C (19a)	1504	2.9 ± 0.1	22 ± 1
B0	$\nu_a(CH_2)$	2918	0.97 ± 0.01	18 ± 2
	$\nu_s(CH_2)$	2850	0.99 ± 0.02	23 ± 2
	C═C (8a)	1608	4.0 ± 0.1	18 ± 1
	C═C (19a)	1495	NA[c]	NA[c]
dP4	$\nu_a(CD_2)$	2195	NA[d]	NA[d]
	$\nu_s(CD_2)$	2090	1.12 ± 0.03	37 ± 2
	C═C (8a)	1612	NA[e]	NA[e]
	C═C (19a)	1514	2.8 ± 0.1	23 ± 1
dB4	$\nu_a(CD_2)$	2195	NA[d]	NA[d]
	$\nu_s(CD_2)$	2090	1.18 ± 0.04	40 ± 3
	C═C (8a)	1608	4.1 ± 0.4	18 ± 1
	C═C (19a)	1501	3.9 ± 0.3	19 ± 1

[a] Dichroic ratio, *D*, is defined as $(A_x + A_z)/(A_y)$. [b] Molecular axes are defined along the C1−C4 axis for the phenyl and biphenyl moieties and at 90° to the methylene C−H bonds for the alkyl chains. [c] Only mode 8a was used to determine the tilt of the biphenyl moiety. [d] Tilt angles for the perdeuterated 14-carbon chains were calculated from the symmetric methylene vibration only. [e] Only mode 19a was used to determine the tilt of the phenyl moiety.

Tilt angles of the phenoxy and biphenoxy groups in capping monolayers of P0 and B0 on OPA were determined from IR modes corresponding to the C−C skeletal deformations of the aryl groups.[26,39−42] The C−C skeletal deformation modes 8a and 19a for para-substituted benzene rings are typically found in the regions of 1570−1628 and 1460−1530 cm^{-1}, respectively.[39] Assuming C_{2v} symmetry for the phenyl and biphenyl groups, these modes have their net transition dipole moments located along the C1−C4 axis of the aryl group. The intensities of these modes in monolayer spectra of P0 and B0 are weak, making quantitative analysis of these bands difficult. To enhance the intensity of these modes, multilayer samples (5−20 bilayers) were used for polarized IR experiments. We observed no structural differences in the early layers as compared to the top layers. Figure 5A shows nonpolarized ATR-FTIR spectra of a five-bilayer sample of P0 on OPA and of a five-bilayer sample of B0 on OPA. The insets in the figure show the C−C skeletal deformation modes of 8a and 19a occurring at 1603 and 1504 cm^{-1}, respectively, for the P0 multilayer sample and occurring at 1608 and 1495 cm^{-1}, respectively, for the corresponding B0 film. Since no bands originating from the zirconated OPA template overlapped with modes 8a or 19a, we were able to use multilayer samples for the measurement of the dichroic ratios for these IR modes. The peak at 1467 cm^{-1} is the alkyl C−H bend mode that contains contributions from both the template and capping monolayers, but it does not distort the aryl modes.

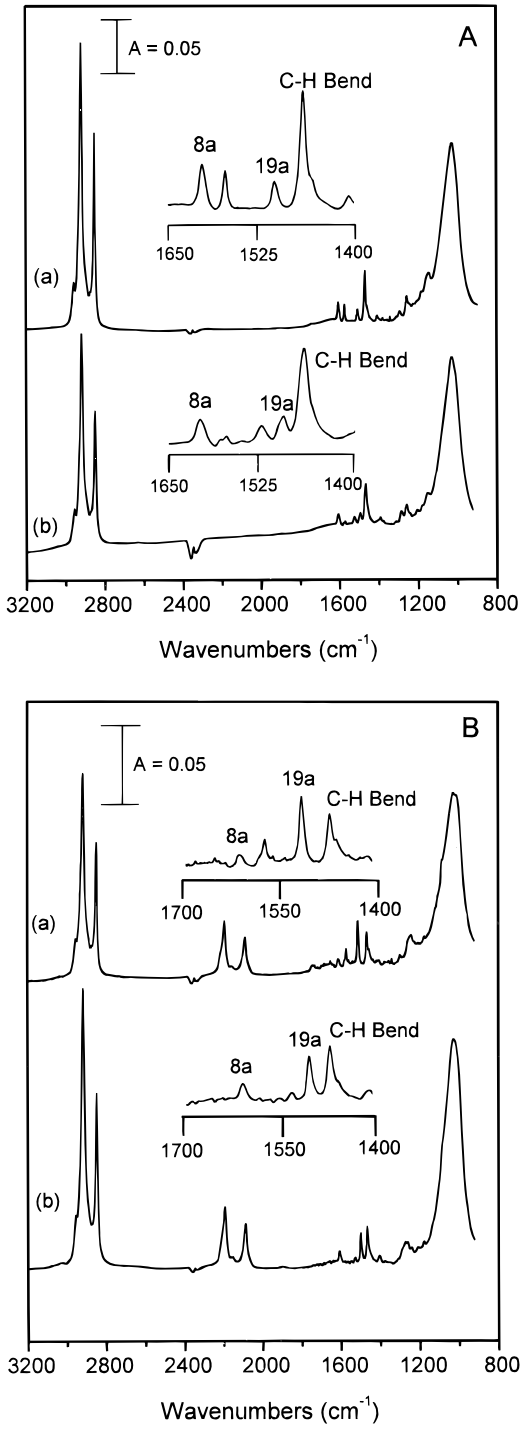

Figure 5. (A) ATR-FTIR spectra of five bilayers of (a) P0 on OPA and (b) B0 on OPA. (B) ATR-FTIR spectra of five bilayers of (a) dP4 on OPA and (b) dB4 on OPA. Insets show an enlarged view of the region containing aryl C−C skeletal deformation modes. Band assignments are discussed in the text.

Figure 6 shows the ATR-FTIR spectra taken in two polarizations of a 15-bilayer sample of P0 on OPA demonstrating how the intensities of modes 8a and 19a change as a function of polarization. The measured dichroic ratios and calculated tilt angles for the aryl moieties are summarized in Table 4 and were determined from samples consisting of 5, 10, and 15 bilayers of P0 on OPA and of B0 on OPA. The measured values did not change as the number of bilayers was increased,

(39) Varsanyi, G. *Vibrational Spectra of Benzene Derivatives*; Academic: New York, 1969.
(40) Tao, Y.-T.; Lee, M.-T.; Chang, S.-C. *J. Am. Chem. Soc.* **1993**, *115*, 9547−9555.
(41) Katon, J. E.; Lippincott, E. R. *Spectrochim. Acta* **1959**, *11*, 627−650.
(42) Steele, D.; Lippincott, E. R. *J. Mol. Spectrosc.* **1961**, *6*, 238−264.

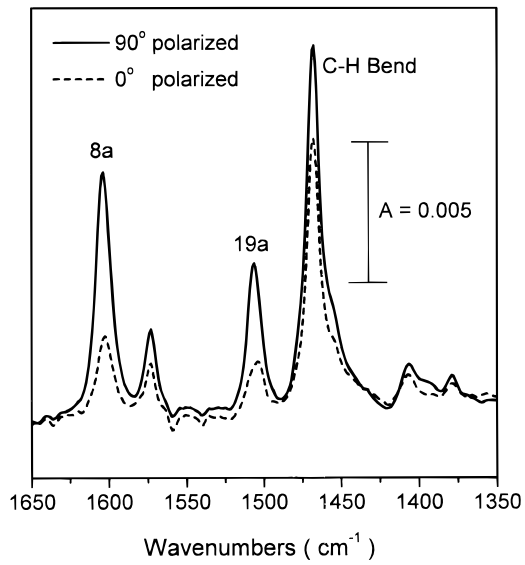

Figure 6. Polarized ATR-FTIR spectra of five bilayers of P0 on an OPA template, taken at 90° and 0° polarization showing the aryl C−C skeletal deformation modes. Superposition of the spectra shows differences in absorbance intensities for the two polarizations.

and the numbers reported in Table 4 are an average of the samples with different numbers of bilayers. Since the transition dipole moment of both skeletal modes is oriented along the same direction, either or both of these modes can be used to calculate the tilt angles of the aryl moieties. For P0 on OPA, both modes were used to determine the tilt angle of 22° for the phenyl group. The long axis of the biphenyl moiety was found to be tilted 18° from the surface normal in films of B0 on OPA. This value was an average over mode 8a alone.

P4 and B4 on an OPA Template. For capping layers of P4 and B4 on OPA, IR spectra revealing the C−H stretch bands are shown in Figure 4. The asymmetric methylene stretch is broadened in each spectrum because contributions from both the 4-carbon and 14-carbon segments overlap in this signal. The peak position of the $\nu_a(CH_2)$ at 2918 cm^{-1} in both cases indicates that there are alkyl chain segments in the P4 and B4 capping monolayers that possess an all-trans conformation. More information can be extracted from these films by looking at the capping monolayers of dP4 and dB4, where the 14-carbon and 4-carbon segments are separated in the IR spectra. The C−D stretch region of capping monolayers on an OPA template of dP4 and dB4 are identical with the C−D stretch regions of the dP4 and dB4 templates, shown in Figure 3. In these IR spectra, the C−D peak positions are nearly identical with those of their solid KBr spectra, with $\nu_a(CD_2)$ and $\nu_s(CD_2)$ appearing at 2195 and 2090 cm^{-1}, respectively. These positions indicate that the 14-carbon alkyl chains are in an all-trans conformation. The narrow fwhm values for the asymmetric methylene vibration of 20 cm^{-1} for both films suggest that the long alkyl chains are close-packed in the films. Table 4 reports the measured dichroic ratios and calculated tilt angles for the 14-carbon alkyl chains in dP4 and dB4. From tilt angle analysis of the symmetric methylene vibration, we found the 14-carbon segments tilt an average of 37° and 40° for dP4 and dB4, respectively. These values are similar to the tilt angles for the 18-carbon chains in the P0 capping layer on an OPA template.

Table 5. Dichroic Ratios,[a] *D*, of IR Modes and the Corresponding Molecular Axis[b] Tilt Angles for the Capping Layers of the P4 and B4 Bilayer Samples

capping monolayer (symmetric)	mode	freq (cm^{-1})	dichroic ratio *D*	tilt angle (deg)
dP4 on P4	$\nu_a(CD_2)$	2195	NA[c]	NA[c]
	$\nu_s(CD_2)$	2090	1.19 ± 0.02	42 ± 2
	C=C (8a)	1612	NA[d]	NA[d]
	C=C (19a)	1514	3.4 ± 0.1	20 ± 1[e]
dB4 on B4	$\nu_a(CD_2)$	2195	NA[c]	NA[c]
	$\nu_s(CD_2)$	2090	1.17 ± 0.01	40 ± 1
	C=C (8a)	1608	3.4 ± 0.2	20 ± 1[e]
	C=C (19a)	1502	3.8 ± 0.2	19 ± 1[e]

[a] Dichroic ratio, *D*, is defined as $(A_x + A_z)/(A_y)$. [b] Molecular axes are defined along the C1−C4 axis for the phenyl and biphenyl moieties and at 90° to the methylene C−H bonds for the alkyl chains. [c] Tilt angles for the perdeuterated 14-carbon chains were calculated from the symmetric methylene vibration only. [d] Only mode 19a was used to determine the tilt of the phenyl ring. [e] Tilt angles for the aryl groups are averaged over the template and capping layers for the symmetric bilayer films.

The tilts of the phenyl and biphenyl moieties were determined from 5, 10, and 15 bilayer samples of dP4 on OPA and dB4 on OPA. Figure 5B shows nonpolarized ATR-FTIR spectra of a five-bilayer sample of dP4 on OPA and of a five-bilayer sample of dB4 on OPA. The insets in Figure 5B show the C−C skeletal deformations with modes 8a and 19a labeled for dP4 at 1612 and 1514 cm^{-1}, respectively, and labeled for dB4 at 1608 and 1502 cm^{-1}, respectively. For dP4 on OPA, mode 19a was used to determine the tilt from the surface normal of 23° for the phenyl group, while both modes were used for finding the 18.5° tilt average of the biphenyl moiety in the capping layer of dB4 on OPA. The reported tilt angles (Table 4) are an average of all the samples studied and were found not to change as the number of bilayers changed.

Symmetric Bilayers of P4 and B4. Symmetric bilayers of P4 on a P4 template and of B4 on a B4 template were also prepared. Again the organization of the different alkyl chain segments was analyzed by studying the partially deuterated molecules. Tilt angles of the 14-carbon segments in capping layers of dP4 and dB4 in the symmetric bilayers are reported in Table 5, along with the tilt angles of the aryl groups in the symmetric bilayers. However, for the symmetric films it was not possible to distinguish the aryl moieties in the templates from those in the capping layers, and the aryl tilt angles listed in Tables 3 and 5 for these bilayers are an average over both the template and capping layers. Polarized IR analysis of the 19a mode for the dP4 symmetric films yielded a tilt for the phenyl group of 20°. The tilt for the biphenyl ring in the symmetric dB4 film is 19.5°, averaged from both modes 8a and 19a.

There are slight differences between the organization of the dP4 and dB4 capping layers in the symmetric bilayers relative to their organization when deposited onto OPA templates. Since the deposition conditions for the capping layers are identical on both templates, the organization of the template must influence the subsequent organization of the capping layer. The largest effect is seen in the four-carbon segment. Figure 7 shows the difference in the C−H stretch modes

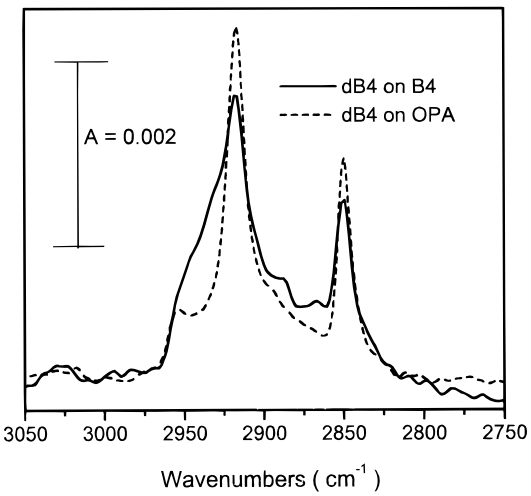

Figure 7. ATR-FTIR spectrum of a capping monolayer of dB4 on a dB4 template superimposed over an ATR-FTIR spectrum of a capping monolayer of dB4 on an OPA template. In each case the capping layer is referenced to the appropriate zirconated template. The peak at 2953 cm^{-1} in the film of dB4 on OPA originates from the methylene unit adjacent to the phosphonate group.[43,44]

between capping layers of dB4 on an OPA template and a dB4 template. Because the material is deuterated, the C−H signal in the spectra is originating from only the four-carbon segments. The $\nu_a(CH_2)$ band is much narrower for the capping layer on the OPA template than on a dB4 template suggesting a more uniform arrangement of the four-carbon segment in the alternating layer film. As discussed above, we believe the four-carbon chains in the templates of dP4 and dB4 to be randomly ordered. Disorder among the phosphonate headgroups in the template directly affects the order in the zirconium layer. When the capping layer is deposited onto an organized zirconium phosphonate surface, as in the zirconated OPA template, the arrangement of the four-carbon segment is more uniform than when the same capping layer is deposited onto the less-organized zirconium phosphonate surface provided by the P4 and B4 templates. The more uniform zirconium phosphonate surface of the zirconated OPA template leads to a better organized capping layer even though the P4 and B4 capping layers are incommensurate with the OPA template layers.

Because the zirconium/phosphonate binding interaction is so strong, the inorganic layer is not expected to be highly crystalline (the crystallinity of solid-state zirconium phosphonates and phosphates is generally quite poor)[45−47] so epitaxy between the capping and template layers is not necessary for good film transfer. The orientation and intermolecular packing of the aryl and 14-carbon segments in dP4 and dB4 show only slight differences when transferred onto both templates, indicating that these segments are less influenced by

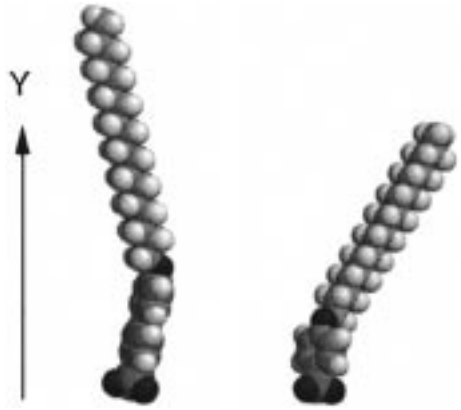

Figure 8. Graphical representation of the organization of the aryl groups and alkyl chains of the capping organophosphonates in alternating films of B0 on OPA and P0 on OPA. In each case, the projection was chosen to show the twist of the phenyl group required to view the measured alkyl chain tilt angles in the plane of the figure. **z**-matrixes were written in HyperChem where they were converted into a Brookhaven Protein Data Bank (PDB) format. Graphical displays of the molecules were achieved using RasMol.[49]

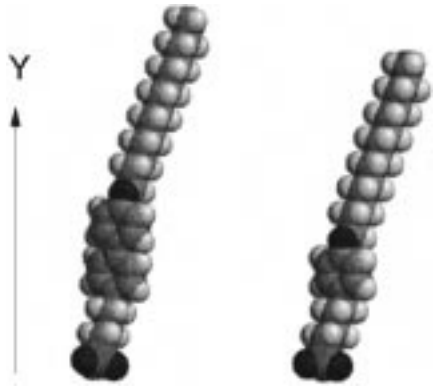

Figure 9. Graphical representation of the organization of the aryl groups and alkyl chains of the capping organophosphonates in alternating films of B4 on OPA and P4 on OPA. In each case, the projection was chosen to show the twist of the phenyl group required to view the measured alkyl chain tilt angles in the plane of the figure. We do not know the orientation of the four-carbon tethers between the aryl and phosphonate groups. They are shown in an all-trans conformation as an example. **z**-matrixes were written and imported into HyperChem where they were converted to a Brookhaven Protein Data Base (PDB) format. Graphical displays of the molecules were achieved using RasMol.

the organization of the zirconated surface. The four-carbon segment buffers the rest of the molecule from the surface, and the packing of the aryl and 14-carbon chain groups is determined by intermolecular forces and not by interactions with the surface.

Structural Analysis. Accumulated data from IR experiments lead to models for the orientations of the aryl phosphonate molecules within the zirconium phosphonate films. The structures shown in Figures 8 and 9 were generated graphically from a **z**-matrix representation of the molecules based on the experimentally determined tilt angles of different segments of each molecule. One possible solution that coordinates the observed tilt angle values with the inherent geometry constraints within the molecules is to allow the aryl group to twist about its C1−C4 axis. The angles determined from polarized IR experiments are with

(43) Bellamy, L. J. *The Infrared Spectra of Complex Molecules*, 3rd ed.; Chapman and Hall: London, 1975.
(44) Frey, B. L.; Hanken, D. G.; Corn, R. M. *Langmuir* **1993**, *9*, 1815−1820.
(45) Alberti, G.; Casciola, M.; Costantino, U.; Vivani, R. *Adv. Mater.* **1996**, *8*, 291−303.
(46) Clearfield, A. *Comm. Inorg. Chem.* **1990**, *10*, 89−128.
(47) Poojary, M. D.; Hu, H.; Campbell, I., F. L.; Clearfield, A. *Acta Crystallogr. B* **1993**, *49*, 996.

Scheme 4. Vectorial Representation of the Molecular Axes of the Aryl and Alkyl Groups

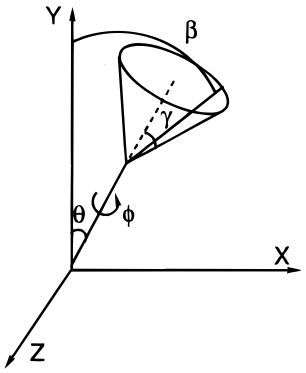

Table 6. Twist Angles (ϕ) for the Aryl Moieties within the Films

monolayer	β^a (deg)	θ^b (deg)	ϕ^c (±2) (deg)
template			
OPA	30	NA[d]	NA[d]
dP4	46	20	±51
dB4	44	19.5	±59
capping			
P0	36	22	±94
B0	20.5	18	±140
dP4 (OPA)	37	23	±93
dB4 (OPA)	40	18.5	±73
dP4 (dP4)	42	20	±69
dB4 (dB4)	40	19.5	±76

[a] β is the tilt of the alkyl chain from the surface normal, as determined from polarized IR experiments. The values reported in this table are the averages from Tables 3−5. [b] θ is the tilt of the aryl moiety from the surface normal, as determined from polarized IR experiments. The values reported in this table are the averages from Tables 3−5. [c] ϕ is obtained from eq 2 ($\cos\beta = \cos\theta\cos\gamma - \sin\theta\cos\phi\sin\gamma$) where $\gamma = 31°$ in all cases. [d] Values of θ and ϕ for OPA are not applicable.

respect to the surface normal. Scheme 4 is a representation of the aryl and alkyl group axes as vectors, where θ is the experimentally determined angle that the C_{2v} axis of the aryl moiety makes with respect to the z axis, β is the experimentally determined tilt angle of the alkyl chain, γ is the angle that the alkyl chain makes with respect to the aryl C_{2v} axis (determined from the internal structure of the molecule and 31° is used here), and ϕ is the angle of rotation about the C_{2v} axis. The relationship between these angles is given by

$$\cos\beta = \cos\theta\cos\gamma - \sin\theta\sin\gamma\cos\phi \qquad (2)$$

As the aryl group is rotated through ϕ from 0° to 180°, the vector representing the alkyl chain will sweep out a cone in which the various positions create different angles with respect to the z axis. For $\theta \sim 20°$ and $\gamma \sim 31°$, a value of $\phi = 0$ gives $\beta = 50°$, while $\phi = 180°$ gives $\beta = 10°$. Our observed β values fall between these two extremes, as can be seen in Table 6. It should be pointed out that this description provides only one possible model for the structure. We have assumed that the bond angle of the ether in the films does not differ from that of an isolated molecule whose ether bond angle was determined from molecular mechanics in HyperChem,[48] and we have assumed that the planes defined by the phenyl ring and the C−O−C bond angle are normal to one another, thus allowing for no rotation of the aryl C−O bond. Also, we are ignoring any orientational constraints imposed by the four-carbon chains since they appear to be disordered in each case. Differences in the twist angle of the aryl groups should be tied to different orientations of the four-carbon segments, or in the cases of P0 and B0, different modes of interaction between the phosphonate headgroup and the zirconium ions. With the present data, details of these interactions cannot be discerned.

On the basis of the analysis described above and the molecular orientations shown in Figures 8 and 9, the orientation of the arylphosphonates does not change significantly from one film to another, with the exception of B0 as the capping layer on an OPA template. Unlike the other molecules, where the long alkyl chain tilts with respect to the normal in the same direction as the aryl group, in the B0 capping layer, the alkyl chain tilts back toward the normal so that the overall tilt of the alkyl chains is much smaller (20.5° in B0 vs 36−46° in the other films). Since the alkyl chains will tilt to maximize van der Waals overlap, and the IR analysis indicates that the alkyl chains are indeed close-packed, these results suggest that the biphenoxy groups are packed more tightly in the B0 film than the phenoxy or biphenoxy groups in any of the other films. The difference in organization of B0 in the transferred film is consistent with the different behavior shown by B0 in the pressure vs area isotherms at the air/water interface. It appears that aggregates of B0 formed at the air/water interface are preserved upon transfer to the zirconated OPA template. As seen in other films,[6,8,9,11] the strong zirconium phosphonate bonding gives the capping layer little opportunity to relax upon transfer under pressure, and the molecular arrangements within the transferred film strongly resemble the structure of the Langmuir monolayer.

The molecular orientation determined in Figures 8 and 9 can be correlated with the layer thicknesses determined by X-ray diffraction. To calculate the length of each molecule, distances of 1.2 Å[26] were used for the length of each CH_2-CH_2 unit on the all-trans alkyl chains, 1.2 Å[26] for the C(alkyl)−O bond length, 2.8 Å[26] for the length of the phenyl rings, 1.8 Å[50] for the C−P bond length, and 1.4 Å[26] for the C(aryl)−O bond length. The P−Zr−P distance is assumed to be 4.4 Å,[47,51] which is the distance observed in crystalline samples of zirconium phenylphosphonates. A distance of 4−5 Å was added to molecule lengths to account for the average van der Waals gap between adjacent layers.[52] The P−Zr−P distance and the van der Waals interlamellar spacing are the values with the largest uncertainties, since these are distances determined for the bulk metal phosphonate solids. Calculated thicknesses of 51 ± 2 Å for P0 on OPA and 58 ± 2 Å for B0 on OPA are in excellent agreement with the measured interlayer

(48) HyperChem, version 4.5. HyperCube, Inc., 419 Phillip Street, Waterloo, Ontario N2L 3X2, Canada.

(49) Sayle, R.; Milner-White, E. J. *RasMol: Biomolecular graphics for all*; Trends Biochem. Sci. **1995**, *20*, pp 333−379.

(50) The value of 1.8 Å for the C−P bond distance was determined from molecular mechanics performed in HyperChem and was used as the value for both C(aryl)−P and C(alkyl)−P bond distances.

(51) Clearfield, A.; Poojary, M. D., private communication.

(52) Frink, K. J.; Wang, R.; Colón, J. L.; Clearfield, A. *Inorg. Chem.* **1991**, *30*, 1438−1441.

distances (Table 2). However, it becomes difficult to extend this approach to films containing P4 and B4 layers because of the disorder in the four-carbon chains. Since we do not know the exact orientation of the four-carbon segment in any of the films, we can calculate a maximum (with a tilt of 0° of the four-carbon segment) and a minimum (with a tilt equal to that of the 14-carbon segment) interlayer spacing in each case. The observed thicknesses are in agreement with the calculated values in each case (Table 2).

Summary

Alternating layer zirconium phosphonate LB films have been prepared from the phenoxy and biphenoxy containing organophosphonates P0, B0, P4, and B4, each alternating with OPA monolayers using a previously developed three-step deposition procedure. Using the same procedure, symmetric bilayer films of P4 and B4 were also constructed. In general, Langmuir monolayers of P4 and B4, where a four-carbon tether separates the aryl group from the phosphonate headgroup, were found to be more processable than the P0 and B0 analogues, where the aryl groups are adjacent to the headgroups. In transferred films, the organization of B0 molecules is significantly different from the organization of the other molecules, which exhibit similar modes of packing. The different orientation of the B0 molecule is attributed to a high degree of aggregation at the air/water interface, which is preserved when the film is transferred to a zirconated template layer. A result of the stepwise deposition method is that the organization of the template layer influences the organization of the capping layer. Capping layers of P4 and B4 are better organized when deposited onto OPA templates than when they are part of the symmetric bilayers P4−Zr−P4 and B4−Zr−B4, respectively. This difference is attributed to a relaxation of the four-carbon segment of the P4 and B4 template layers, which is maintained after zirconation providing a less-organized zirconium phosphonate surface for depositing the capping layer.

Because of the strength of the metal−headgroup interactions, zirconium phosphonate films provide a viable approach to the formation of extremely stable LB assembles. This study demonstrates that zirconium phosphonate-based LB films can be prepared from groups different than simple alkylphosphonates. Increasingly sophisticated organophosphonates should lead to functionalized organic/inorganic metal phosphonate LB films.

Acknowledgment. We are grateful to the National Science Foundation for financial support. M.A.P. thanks the National Science Foundation for a predoctoral fellowship. We thank Jerry L. Reddinger for helpful synthetic advice and Ted A O'Brien for help with the analyses of molecular orientation. Special thanks are given to the University of Florida Major Analytical Instrumentation Center for use of the X-ray and XPS facilities.

Supporting Information Available: Full synthetic experimental details, including characterization for each acid and intermediate, and the complete derivation of eq 2 (17 pages). Ordering information is given on any current masthead page.

CM9703379